

This document is confidential and is proprietary to the American Chemical Society and its authors. Do not copy or disclose without written permission. If you have received this item in error, notify the sender and delete all copies.

Immobilization of Privileged Triazolium Carbene Catalyst for Batch and Flow Stereoselective Umpolung Processes

Journal:	<i>ACS Catalysis</i>
Manuscript ID	cs-2017-021644.R2
Manuscript Type:	Article
Date Submitted by the Author:	n/a
Complete List of Authors:	Ragno, Daniele; Università di Ferrara, Chemical and Pharmaceutical Sciences Di Carmine, Graziano; Università degli Studi di Ferrara Dipartimento di Scienze Chimiche e Farmaceutiche, Organic Chemistry Brandolese, Arianna; University of Ferrara, Department of Chemistry and Pharmaceutical Sciences Bortolini, Olga; University of Ferrara, Department of Chemistry Giovannini, Pier Paolo; University of Ferrara, Department of Chemistry and Pharmaceutical Sciences Massi, Alessandro; University of Ferrara, Department of Chemistry and Pharmaceutical Sciences

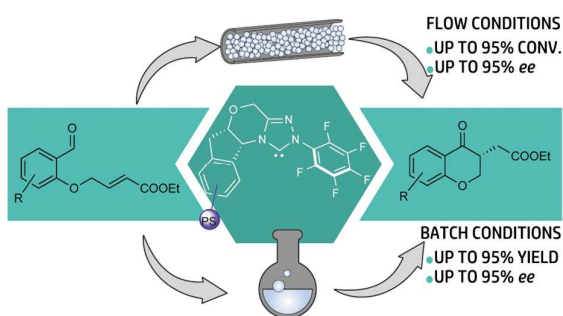
SCHOLARONE™
Manuscripts

Immobilization of Privileged Triazolium Carbene Catalyst for Batch and Flow Stereoselective Umpolung Processes

Daniele Ragno, Graziano Di Carmine, Arianna Brandolese, Olga Bortolini, Pier Paolo Giovannini, and Alessandro Massi*

Dipartimento di Scienze Chimiche e Farmaceutiche, Università di Ferrara, Via Luigi Borsari, 46, I-44121 Ferrara (Italy)

alessandro.massi@unife.it



Abstract: A strategy for the immobilization of the valuable triazolium carbene Rovis catalyst onto polystyrene and silica supports is presented. Initially, the catalyst activity and recyclability were tested under batch conditions in the model stereoselective intramolecular Stetter reaction leading to optically active chromanones. Good results in terms of yield (95%) and enantioselectivity (ee: 81-95%) were detected for the polystyrene-supported catalyst (10 mol%), while poorer results were collected for the silica-supported analogue. Also, continuous-flow experiments were performed by fabricating the corresponding polystyrene monolithic microreactors (pressure-resistant stainless-steel columns) to prove the benefits of the heterogeneous catalysis and the flow regime observing a high stability of the catalytic bed (48 h) with unaltered conversion efficiency and stereoselectivity.

Keywords: enantioselective catalysis, chiral N-heterocyclic carbenes, polystyrene-supported catalysts, flow chemistry, organocatalysis

Introduction

The broad application of N-heterocyclic carbene (NHC) organocatalysts have been extensively demonstrated in a number of research programs,¹ including those devoted to the total synthesis of biologically relevant chiral products.² Indeed, the impressive levels of stereocontrol exerted by chiral NHCs together with the easy access to unconventional synthetic strategies represent competitive advantages related to the use of this class of catalysts. The poor stability to air and moisture, the elevated cost and/or the difficult preparation may, however, hamper the effective application in industrial processes of chiral NHCs, which are often quite complex molecules. The synthetic platform based on heterogeneous catalysis, eventually in microstructured flow reactors,³ may constitute a solution to overcome the above limitations offering advantages in terms of catalyst activity/stability, productivity, sustainability, and costs.⁴

Intensive research has been recently carried out on the fixation of NHCs on solid and soluble supports by different immobilization strategies for studies in the fields of organic and organometallic chemistry.⁵ With particular reference to the use of NHCs as organocatalysts, in 2004 the group of Barret reported on Stetter reactions promoted by a ROMPgel-supported thiazolium iodine pre-catalyst.⁶ An imidazole-based polystyrene was later presented by Storey and Williamsons to perform benzoin reactions.⁷ Zeitler and co-workers introduced different NHC precursors immobilized on MeOPEG for intramolecular Stetter reactions and redox esterifications.⁸ Additionally, poly-NHCs were successfully utilized in ketone/imine hydrosilylation,⁹ silane alcohol condensation,⁹ and benzoin reaction.^{10,11} Imidazolium-functionalized crosslinked element organic frameworks were also tested as efficient pre-catalysts in the conjugated umpolung of α,β -cinnamaldehyde.¹² The group of Taton deeply contributed to this area of research by reporting on the preparation of highly stable poly-NHC-CO₂ adducts and poly(ionic liquid)-based polymeric catalysts.¹³ Very recently, NHCs supported on vinylic addition polynorbornene were presented for the synthesis of γ -butyrolactones and saturated esters,¹⁴ while azolium salt pre-catalysts supported onto silica and polystyrene were demonstrated to efficiently catalyze the self-couplings of furfural and 5-HMF.¹⁵ To the best of our knowledge, however, only one example is reported in the literature dealing with the immobilization of enantiomerically pure NHCs.¹⁶ The group of Glorius supported a (*R*)-binol-derived imidazolium salt on Fe₃O₄ nanoparticles for the asymmetric allylation of 4-nitrobenzaldehyde detecting, however, a moderate level of stereoselectivity and the impossibility of catalyst recovery by magnetic decantation.¹⁶

Surprisingly, the combination of microreactor technology with umpolung catalysis is still a poorly investigated field of research. Monbaliu and co-workers developed a suitable continuous-flow apparatus for the generation of free NHCs under homogeneous conditions and their subsequent

utilization as organocatalysts by the reaction telescoping approach.¹⁷ Undivided microfluidic electrolysis cells were described by the group of Brown for the oxidative esterification and amidation of aldehydes promoted by homogeneous NHCs.¹⁸ In the area of heterogeneous umpolung catalysis, Lupton and-coworkers developed fixed-bed reactors packed with an immobilized imidazolidinium pre-catalyst for the synthesis of biodiesel.¹⁹ Our group also contributed to this field reporting on the fabrication of thiazolium-functionalized polystyrene monolithic columns to perform racemic benzoin, Stetter and acyloin-type reactions in flow mode.²⁰ In addition, packed-bed bioreactors filled with a thiamine diphosphate-dependent enzyme supported on mesoporous silica were operated in our laboratories for the continuous production of optically active tertiary alcohols by the umpolung strategy.²¹ More recently, we disclosed a practical procedure based on a double electron-transfer process for the polarity reversal of 1,2-diketones using fixed-bed reactors packed with a suitable polystyrene-supported phosphazene base.²²

Herein, we report on the immobilization onto polystyrene and silica supports of the enantiomerically pure triazolium carbene Rovis catalyst that is a 'privileged' promoter for a variety of highly stereoselective processes (Figure 1).^{1d,23} Once demonstrated the excellent activity of the polystyrene-supported version of the Rovis catalyst in bath experiments, this study culminated with the fabrication of polystyrene monolithic columns, which displayed in model intramolecular Stetter reactions high levels of conversion efficiency (up to 95%) and enantioselectivity (up to 95%) together with a remarkable stability of the catalytic bed (2 days on stream).

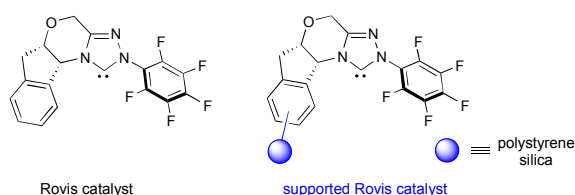


Figure 1. Rovis catalyst and heterogeneous versions thereof.

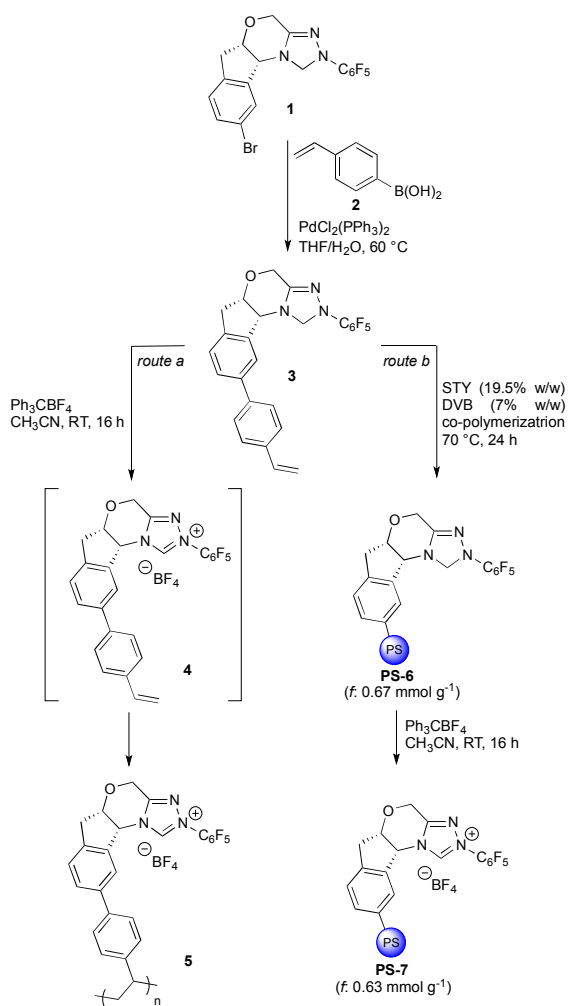
Results and discussion

Our study commenced with the design of an effective immobilization strategy for supporting the Rovis catalyst onto both polystyrene and silica supports by a divergent synthetic approach. Additional goals were the achievement of the excellent levels of activity and stereocontrol displayed by the homogeneous catalyst together with a good recyclability of the supported counterparts. We were aware of previous studies reporting on the lower activity of heterogeneous NHCs prepared by direct N-alkylation of the azole unit with chloromethylated supports;²⁴ hence,

1
2
3 we reasoned that the introduction through a covalent linkage of a quite flexible spacer between the
4 phenyl ring of the indanyl moiety and the heterogeneous matrix could be advantageous for our
5 purposes. The group of Bode first described the selective bromination of the *cis*-aminoindanol
6 backbone as a route for the fine tuning of catalyst structure/activity;²⁵ later on, Rovis and co-
7 workers demonstrated that halo-indanol triazolines were suitable substrates for the diversification of
8 triazolium-based NHC catalysts via Suzuki-Miyaura cross-coupling followed by trityl cation-
9 mediated oxidation to the corresponding triazolium salts.²⁶ Inspired by these works, our
10 immobilization strategies started with the multi-gram scale synthesis of the known 6-bromo
11 triazoline **1** (Scheme 1).^{26,27} Next, the key styryl adduct **3** was prepared in 60% yield by the Suzuki-
12 Miyaura cross-coupling of **1** with 4-vinylphenylboronic acid **2** (1.5 equiv.) under optimal conditions
13 [K_3PO_4 (2 equiv.), $Pd(PPh_3)_2Cl_2$ (5 mol%), THF-H₂O, 60 °C, 4 h). The vinylated triazoline **3** was
14 then subjected to the trityl cation-based oxidation procedure^{26,28} [Ph_3CBF_4 (1 equiv.), CH₃CN, RT,
15 16 h) to access the corresponding triazolium salt **4** and, subsequently, the polystyrene resin **PS-7** by
16 copolymerization with styrene and divinylbenzene (route a). Surprisingly, the oxidation step was
17 accompanied by the homopolymerization of **4** affording the poly-(triazolium) pre-catalyst **5** in
18 almost quantitatively yield. While this derivative proved to be quite effective in the model
19 stereoselective Stetter reaction (see Table 1, entry 15), at this stage of our study no further
20 investigations were carried out to determine the molecular weight and dispersity of **5** because of the
21 impossibility of recycling it by precipitation or centrifugation techniques.
22
23

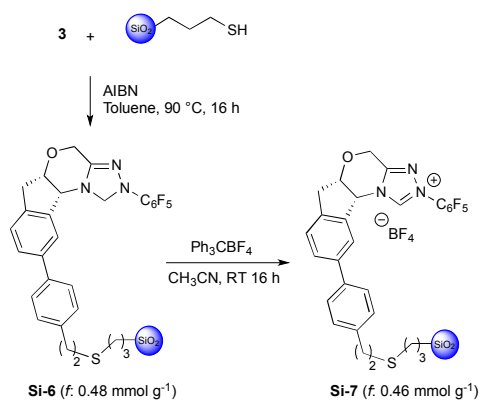
24 Therefore, the triazoline to triazolium conversion was next investigated in the heterogeneous phase
25 after preparation of the triazoline-functionalized polystyrene resin **PS-6** (route b). Taking into
26 consideration that an important goal of our research was the set-up of an effective flow procedure as
27 well, the polymerization study of the styryl triazoline **3** was performed with the aim to prepare the
28 polystyrene resin **PS-6** in the form of monolithic columns,²⁹ which are known to display improved
29 flow characteristics compared to randomly packed reactors.³⁰ Accordingly, the polymerization
30 mixture was molded in both glass and stainless-steel columns (4.6 mm internal diameter, 10 cm
31 length) in parallel experiments in order to evaluate, in the first case, the macroporous nature and
32 loading of the polymeric material, and, in the second case, the flow-through behavior of the column.
33 Hence, the composition of the polymerization mixture was optimized as follow: **3** (13% w/w),
34 styrene (19.5% w/w), DVB (7% w/w), 1-dodecanol (50% w/w) and Toluene (10% w/w) as the
35 porogens, and AIBN (0.5% w/w) as the radical initiator (Scheme 1). The polymerization (70 °C, 24
36 h) proved to be very reproducible affording **PS-6** with a satisfactory loading of triazoline units (*f*:
37 0.67 mmol g⁻¹). Afterwards, the triturated monolith was suspended in dry acetonitrile and treated
38 with an excess of trityl tetrafluoroborate (3 equiv.) for 16 hours. Satisfyingly, the target triazolium-
39
40
41
42
43
44
45
46
47
48
49
50
51
52
53
54
55
56
57
58
59
60

functionalized resin **PS-7** (f : 0.63 mmol g^{-1}) was obtained with excellent conversion (>95%) as determined by quantitative 1H NMR analysis (internal standard) of the supernatant solution containing the diagnostic by-product triphenylmethane.



Scheme 1. Synthesis of triazolium-functionalized resin **PS-7**.

The silica-supported pre-catalyst **Si-7** was prepared by a similar immobilization-oxidation strategy starting from suitably prepared mercaptopropyl silica gel³¹ and the vinylated triazolone **3** as depicted in Scheme 2. Thus, under standard thermal conditions (AIBN, 90 °C, 16 h), the triazolone-functionalized silica **Si-6** was produced with a suitable level of functionalization (f : 0.48 mmol g^{-1}) detecting the complete disappearance of the SH stretching band at 2580 cm^{-1} (FT-IR analysis). Finally, the trityl cation-based oxidation procedure afforded the triazolium-functionalized silica **Si-7** (f : 0.41 mmol g^{-1}) with a satisfactory level of conversion efficiency (82%).



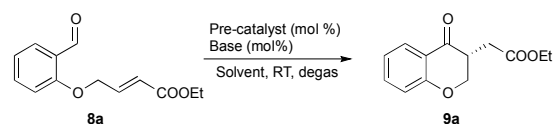
21
22
23
24
25
26
27
28
29
30
31
32
33
34
35
36
37
38
39
40
41
42
43
44
45
46
47
48
49
50
51
52
53
54
55
56
57
58
59
60

Scheme 2. Synthesis of triazolium-functionalized silica **Si-7**.

The stereoselective intramolecular Stetter reaction leading to optically active chromanones **9**³² was selected as the benchmark to test the catalytic activity and recyclability of the newly prepared heterogeneous Rovis pre-catalysts **PS-7** and **Si-7** (Table 1). To our delight, application of the reaction conditions previously optimized for the homogeneous counterpart,^{32f} using 20 mol% of **PS-7** in the presence of KHMDS as the base (20 mol%; Toluene, RT, 16 h) under degassed conditions (Ar) gave **9a** in excellent yield (95%) and enantioselectivity (92% ee; entry 1). Lowering the catalyst loading to 10 mol% left unchanged the reaction outcome (entry 2), thus indicating an even superior activity of the polystyrene-supported pre-catalyst **PS-7** compared to the homogeneous counterpart; a further decrease of the catalyst loading (5 mol%) resulted in a lower yield of chromanone **9a** (63%), which was recovered with unaffected enantiomeric excess (entry 3). Keeping in mind the subsequent execution of flow experiments, different soluble organic bases were also screened in the model reaction. Triethylamine furnished **9a** in slightly lower yield (80%) but improved enantioselectivity (94% ee, entry 4), whereas the use of DBU determined a partial erosion of stereocontrol (90% ee; entry 5). The solvent effect was next considered utilizing KHMDS or triethylamine as the preferred bases; it was found a diminished activity of **PS-7** in pentane and ethanol (entries 6-7), whereas the use of either DMF or the ecofriendly phosphate buffer (pH 8.5)/ethanol mixture completely inhibited the catalyst activity (entries 8-9). Lastly, when temperature was decreased to 0 °C, **9a** was recovered with improved stereoselectivity (94% ee) but lower yield (35%; entry 10); by contrast, a temperature increase (50 °C) guaranteed the full conversion of **8a** with 5 mol% of **PS-7** accompanied, however, by a slight decrease of enantioselectivity (90% ee; entry 11). Unexpectedly, much poorer results were achieved using the silica-supported pre-catalyst **Si-7**, likely because of its higher sensibility to moisture compared to **PS-7**. A number of solvent/base combinations were screened (also in the presence of molecular

sieves), being Toluene/KHMDS the most effective one (**9a**: 45%; 93% ee, entry 12). As far as the recyclability of **PS-7** is concerned, a substantial maintenance of enantioselectivity was detected after ten cycles with only a moderate decrease (ca. 5%) of conversion efficiency after each recycle (filtration and washing of the resin with ethyl acetate; entries 13-14). Overall, these results confirmed the effectiveness of **PS-7**, which showed an accumulated turnover number (TON) of 70 under batch conditions.

Table 1. Screening of reaction conditions with **PS-7** and **Si-7**.^a



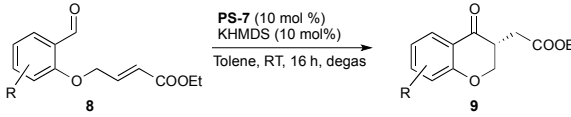
Entry	Pre-Catalyst (mol%)	Solvent	Base	Yield ^b (%)	ee ^c (%)
1	PS-7 (20)	Toluene	KHMDS	95	92
2	PS-7 (10)	Toluene	KHMDS	95	93
3	PS-7 (5)	Toluene	KHMDS	63	93
4	PS-7 (10)	Toluene	NEt ₃	85	94
5	PS-7 (10)	Toluene	DBU	86	90
6	PS-7 (10)	Pentane	KHMDS	75	92
7	PS-7 (10)	EtOH	NEt ₃	62	90
8	PS-7 (10)	DMF	NEt ₃	-	-
9 ^d	PS-7 (10)	EtOH	Buffer	-	-
10 ^e	PS-7 (10)	Toluene	KHMDS	35	94
11 ^f	PS-7 (5)	Toluene	KHMDS	95	90
12	Si-7 (10)	Toluene	KHMDS	45	93
13 ^g	PS-7 (10)	Toluene	KHMDS	64	92
14 ^h	PS-7 (10)	Toluene	KHMDS	38	91
15	5 (10)	Toluene	KHMDS	70	92

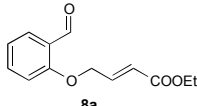
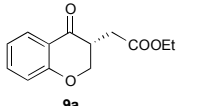
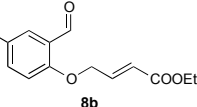
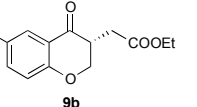
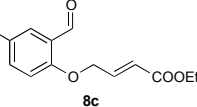
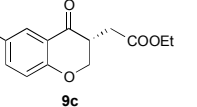
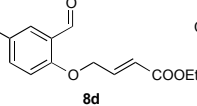
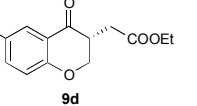
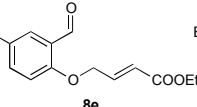
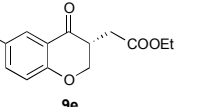
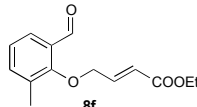
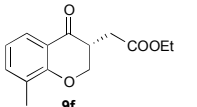
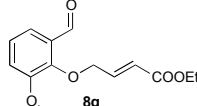
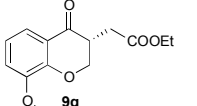
^aReactions carried out with 0.12 mmol of **8a** in 1 mL of solvent under degassed conditions; base was equimolar to the pre-catalyst. ^bIsolated yield. ^cDetermined by chiral HPLC analysis. ^dReaction performed in a 1:1 mixture of EtOH and phosphate buffer (pH 8.5). ^eReaction run at 0 °C. ^fReaction run at 50 °C. ^g5th recycle. ^h10th recycle.

After having established the superior activity of **PS-7**, the scope of the intramolecular Stetter reaction was investigated under the optimized batch conditions (**PS-7** 10 mol%; KHMDS 10 mol%; Toluene, RT, 16 h). Accordingly, different Michael acceptors **8** displaying electron-withdrawing and electron-donating groups at 3- and 5-position of the aromatic ring were tested detecting results comparable to those reported for the homogeneous catalyst (Table 2).^{32f} In particular, substrates **8** with electron-donating groups at 5-position were converted into the corresponding chromanones **9** with good yields and enantioselectivities (entries 2-3). Substitution at the same position with electron-withdrawing groups led to an increase of conversion efficiency (95% yield, 4.5 h reaction time) with maintenance of stereoselectivity (entries 4-5). Finally, in analogy with the homogeneous batch study,^{32f} the presence of electron-donating groups at 3-position determined a partial loss of

enantioccontrol by the supported catalyst **PS-7** (entries 6-7). Nevertheless, variation of the enantiomeric excess of products **9** because of partial epimerization cannot be excluded.

Table 2. Reaction scope with **PS-7** under batch conditions.^a

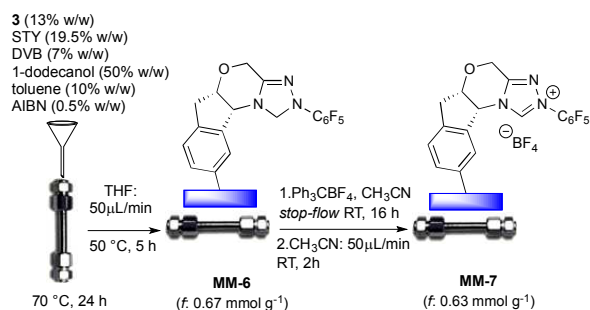


Entry	Substrate	Product	Yield (%) ^b	ee (%) ^c
1			95	93
2			95	95
3			95	90
4			95 ^d	92
5			95 ^d	92
6			95	81
7			95	90

^aReactions run with 0.24 mmol of **8**. ^bIsolated yield. ^cDetermined by chiral HPLC. ^dReaction time: 4.5 h.

Encouraged by the excellent activity displayed by **PS-7** under batch conditions and driven by our experience on the detected superior stability of polystyrene-supported azolium carbene catalysts in flow regime,²⁰ we next investigated the performance of **PS-7** as a monolithic microreactor (hereafter designed as **MM**). Hence, the optimized polymerization mixture containing the triazoline monomer **3** was charged into the stainless-steel column, which was warmed at 70 °C for 24 hours (Scheme 3). After cooling, the resulting monolithic column **MM-6** was thoroughly washed with THF to remove non-polymeric materials and the porogens. Afterwards, the stop-flow reaction

technique was applied for the preparation of the triazolium-functionalized monolith **MM-7**. Accordingly, a 0.5 M solution of trityl tetrafluoroborate in anhydrous acetonitrile was pumped inside the column, which was then sealed and kept at room temperature for 16 hours. After washing with acetonitrile, the above operation was repeated twice to ensure a complete derivatization of the monolith as detected by ^1H NMR analysis of the eluate containing the triphenylmethane by-product. In addition, pycnometry allowed the determination of the dead volume (V_0) and total porosity (ϵ_{tot}) of **MM-7**, while the SEM analysis confirmed the macroporous nature of the monolithic column (Figure 2).



	loaded 3 [mmol] ^a	V_G [mL] ^b	V_0 [mL] ^c	Total Porosity ^d	Time [min] ^e	Pressure [bar] ^f
MM-7	0.40	1.66	1.32	0.80	132	2

^aDetermined by elemental analysis and expressed as mmol of pyrrolidiny-tetrazole units per gram of functionalized resin. ^bGeometric volume of the stainless-steel column. ^cVoid volume determined by pycnometry. ^dTotal porosity = V_0/V_G . ^eResidence time calculated at 10 $\mu\text{L}/\text{min}$. ^fBackpressure measured at 20 $\mu\text{L}/\text{min}$ (RT, THF).

Scheme 3. Fabrication and main features of monolithic microreactor **MM-7**.

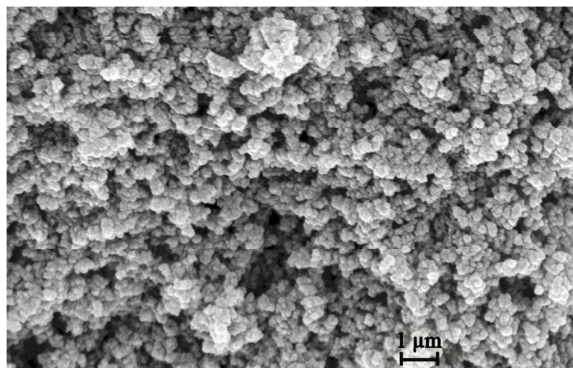
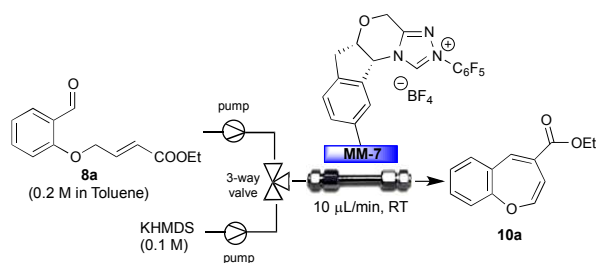


Figure 2. SEM picture of macroporous **MM-7**.

Continuous-flow experiments were carried out with the two-pump, three-way valve system depicted in Scheme 4. Microreactor **MM-7** was independently fed at $10 \mu\text{Lmin}^{-1}$ with continuously degassed solutions in Toluene of the Michael acceptor **8a** (0.2 M) and KHMDS (0.1 M). Disappointingly, after the achievement of the steady-state regime (ca. 3 h), analysis of the outlet stream ($^1\text{H NMR}$) showed a very poor conversion in **9a** with formation of the ester **10a** as the main reaction product. This result clearly indicated that the strong base KHMDS reacted preferentially with the substrate **8a** affording **10a** through a tandem olefin isomerization-crotonation reaction.^{32a} Similar reaction outcomes were also observed with lower concentrations of the KHMDS solution (up to 0.01 M). The use of a stoichiometric amount of KHMDS (0.40 mmol) to pre-activate the supported triazolium salt pre-catalyst was also attempted. Unfortunately, this experiment produced a very low conversion (5%) in **9a** during the first hour of the flow process together with the recovery of the unreacted aldehyde **8a**. This result was in agreement with our previous findings on the need for a constant basic medium to successfully perform umpolung catalysis in flow regime.²⁰



Scheme 4. Set-up for the continuous-flow experiments and reaction outcome using KHMDS as the base.

Opportunely, the batch optimization study (Table 1, entry 4) suggested us the utilization of the weaker triethylamine base for the generation of the active triazolium carbene species under flow conditions. Thus, a preliminary control batch experiment was conducted with **8a** in the presence of the sole triethylamine to exclude the occurrence of the undesired side-reaction with this base. Then, the flow process was optimized with a two-fold excess of triethylamine (0.4 M solution) allowing the production of **9a** with a satisfactory instant conversion (90%) and excellent enantioselectivity (94% ee; flow rate: $10 \mu\text{Lmin}^{-1}$; Table 3, entry 1). Nevertheless, the most striking result of this experiment was the long-term stability of monolith **MM-7**, which could be operated for 48 hours with unaltered values of conversion and stereoselectivity. Significantly, 120 hours operation determined a loss of only half the initial productivity (Figure 3). These findings correspond to a total TON of 132 and a two-fold increase of productivity moving from batch to flow conditions,

thus demonstrating the beneficial role of the flow regime due to the continuous removal of moisture and trace impurities from the catalytic bed.

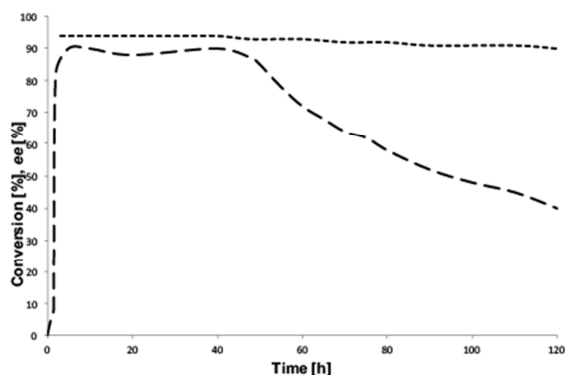
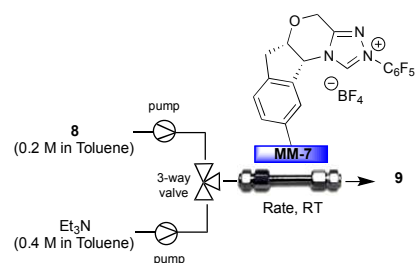


Figure 3. Long-term stability of the monolithic column **MM-7** in the flow synthesis of **9a**. Conversion [%], dashed line; ee [%], dotted line.

The continuous production of chromanones **9b-g** was finally examined under the optimized flow conditions (Table 3, entries 2-7). Flow rates were adjusted to reach elevated conversion efficiencies (>90%) for an easier downstream purification of the reaction products. Overall, chromanones **9** were obtained with satisfactory productivities (ca. 0.1-0.3 mmol h⁻¹ mmol_{cat}⁻¹) and unmodified enantioselectivity compared to the batch process.

Table 3. Continuous-flow production of chromanones **9** with monolithic microreactor **MM-7**.^a



Entry	Product (conv. [%]) ^b	ee ^c (%)	Rate ($\mu\text{L min}^{-1}$)	P^d
1	9a (90)	94	10	138
2	9b (92)	95	10	141
3	9c (91)	90	10	140
4	9d (95)	92	20	292
5	9e (95)	92	20	292
6	9f (90)	81	10	138
7	9g (92)	90	10	141

^aSee the experimental section for a description of the flow apparatus. ^bInstant conversion in the steady-state regime as established by ¹H NMR analysis. ^cDetermined by chiral HPLC. ^dProductivities (P) are measured in mmol(product) h⁻¹ mmol(cat)⁻¹ × 10³.

Conclusions

In summary, we have presented a polystyrene-supported version of the valuable Rovis triazolium carbene catalyst, which has been proven to be highly active in model intramolecular Stetter reactions with levels of conversion efficiency and enantioselectivity comparable to those displayed by the homogenous counterpart. A good recyclability of the heterogeneous catalyst was observed in batch experiments, while an improved stability was detected in flow regime using the supported Rovis catalyst in the form of monolithic column. To the best of our knowledge, this study represents the first example of immobilization of chiral NHC catalysts for the successful execution of stereoselective processes under batch and flow conditions, thus paving the way for further progress in the field of asymmetric catalysis by the umpolung strategy.

Experimental section

All moisture-sensitive reactions were performed under an argon atmosphere using oven-dried glassware. Solvents were dried over a standard drying agent and freshly distilled prior to use. Reactions were monitored by TLC on silica gel 60 F₂₅₄ with detection by charring with potassium permanganate and/or phosphomolybdic acid. Flash column chromatography was performed on silica gel 60 (230-400 mesh). Optical rotations were measured at 25 ± 2 °C in the stated solvent; $[\alpha]_D$ values are given in 10⁻¹ deg cm² g⁻¹ (concentration *c* given as g/100 mL). ¹H (300 MHz), ¹³C (101 MHz) and ¹⁹F (376 MHz) NMR spectra were recorded in CDCl₃ or acetone-*d*₆ solutions at room temperature. The chemical shifts in ¹H and ¹³C NMR spectra were referenced to trimethylsilane (TMS). The chemical shifts in ¹⁹F NMR spectra were referenced to CFCl₃. Peak assignments were aided by ¹H-¹H COSY and gradient-HMQC experiments. Enantiomeric excess (ee) were evaluated by HPLC using Lux amylose 2 or Lux Cellulose 2 columns. FT-IR analyses were performed using the Bruker Instrument Vertex 70. Elemental analyses were performed using a FLASH 2000 Series CHNS/O analyzer (ThermoFisher Scientific). SEM analyses were performed using a Zeiss Gemini 1530 scanning electron microscope. For high resolution mass spectrometry (HRMS) the compounds were analyzed in positive ion mode using an Agilent 6520 HPLC-Chip Q/TOF-MS (nanospray) with a quadrupole, a hexapole, and a time of flight unit to produce the spectra. The capillary source voltage was set at 1700 V; the gas temperature and drying gas were kept at 350 °C and 5 L min⁻¹, respectively. The MS analyzer was externally calibrated with ESI-L low concentration tuning mix from *m/z* 118 to 2700 to yield accuracy below 5 ppm. Accurate mass data were collected by directly infusing samples in 40/60 H₂O/ACN 0.1% TFA into the system at a flow rate of 0.4 μL min⁻¹. Triazolone **1** was synthesized according to literature procedures.^{26,27} Mercaptopropyl silica gel was prepared according to a literature procedure.³¹ Starting aldehydes **8a-**

1
2
3 **8g** where synthesized as described.³³ All racemates were synthesized using 6,7-dihydro-2-
4 pentafluorophenyl-5*H*-pyrrolo[2,1-*c*]-1,2,4-triazolium tetrafluoroborate (CAS 862095-91-8,
5 purchased by Sigma Aldrich) as the catalyst. Absolute stereochemistry for chromanones **9a-9g** was
6 determined by comparison of the measured optical rotation value with the corresponding literature
7 data.^{32f}
8
9
10

11
12
13 **(5*aS*,10*bR*)-2-(perfluorophenyl)-9-(4-vinylphenyl)-1,2,4,5*a*,6,10*b*-hexahydroindeno[2,1-
14 *b*][1,2,4]triazolo[4,3-*d*][1,4]oxazine (**3**).**

15
16 Triazoline **1**²⁶ (0.34 g, 0.75 mmol), PdCl₂(PPh₃)₂ (24 mg, 0.037 mmol, 5 mol%), boronic acid **2**
17 (0.17 g, 1.12 mmol), and potassium phosphate (0.32 g, 1.5 mmol) were loaded into a glass vial.
18 Subsequently, anhydrous THF (5 mL) was added, followed by degassed water (1.7 mL). The
19 mixture was degassed under vacuum, and saturated with argon (by an Ar-filled balloon) three times.
20 Subsequently, the vial was sealed and the reaction mixture was stirred at 60 °C. After 4 hours,
21 complete conversion of starting material was detected by TLC. The reaction was then cooled to
22 room temperature, quenched with water (4 mL), and extracted with EtOAc (2 × 5 mL). The
23 combined organic phases were dried over Na₂SO₄, concentrated, and eluted from a column of basic
24 alumina with 5:1 cyclohexane-EtOAc to give triazoline **3** (218 mg, 60%) as a pale yellow
25 amorphous solid. [α]_D²⁵ = -42.0 (*c* = 1.0, acetone). ¹H NMR (300 MHz, acetone-*d*₆) δ = 7.72 (m,
26 1H, Ar), 7.65 (m, 2H, Ar_{Sty}), 7.60 (m, 1H, Ar), 7.53 (m, 2H, Ar_{Sty}), 7.41 (m, 1H, Ar), 6.79 (dd, *J*₁₋
27 *Sty*,_{2*a*-Sty} = 17.7, *J*_{1-*Sty*,2*b*-Sty} = 11.0 Hz, 1H, H-1_{Sty}), 5.85 (dd, *J*_{1-*Sty*,2*a*-Sty} = 17.7, *J*_{2*a*-Sty,2*b*-Sty} = 0.9 Hz,
28 1H, H-2*a*_{Sty}), 5.67 (m, 1H, H-3*a*_{Tr}), 5.25 (dd, *J*_{1-*Sty*,2*b*-Sty} = 11.0, *J*_{2*a*-Sty,2*b*-Sty} = 0.9 Hz, 1H, H-2*b*_{Sty}),
29 5.04 (m, 1H, H-3*b*_{Tr}), 4.77 (dd, 1H, *J*_{4*Ind*,5*Ind*} = 10.0, *J*_{5*Ind*,10*Ind*} = 5.6 Hz, 1H, H-5*Ind*), 4.61 (d, *J*_{2*a*Oxa,}
30 _{2*b*Oxa} = 15.6 Hz, 1H, H-2*a*_{Oxa}), 4.56 (d, *J*_{5*Ind*,10*Ind*} = 5.6 Hz, 1H, H-10*Ind*), 4.46 (d, *J*_{2*a*Oxa,}
31 _{2*b*Oxa} = 15.6 Hz, 1H, H-2*b*_{Oxa}), 3.30-3.24 (m, 2H, H-4*Ind*); ¹³C NMR (101 MHz, acetone-*d*₆) δ = 149.0 (C=N),
32 141.7 (C), 140.3 (C), 139.7 (C), 139.7 (C), 136.6 (CH), 136.4 (CH-1_{Sty}), 127.1 (2 CH), 126.6 (2
33 CH), 125.7 (CH), 125.6 (C), 123.1 (CH), 113.3 (CH₂-2_{Sty}), 77.1 (CH-5*Ind*), 73.6 (CH₂-3_{Tr}), 62.3
34 (CH-10*Ind*), 59.2 (CH₂-2_{Oxa}), 34.9 (CH₂-4*Ind*); ¹⁹F NMR (376 MHz, acetone-*d*₆) δ = -151.1 (m, 2F, *o*-
35 F), -166.1 (m, 2F, *m*-F), -166.5 (m, 1F, *p*-F). HRMS (ESI/Q-TOF) calcd for C₂₆H₁₉F₅N₃O ([M +
36 H]⁺) 484.1443, found: 484.1450.
37
38
39
40
41
42
43
44
45
46
47
48
49
50

51
52
53 **Poly-(triazolium) salt (**5**).**

54 A vigorously stirred mixture of styryl functionalized triazoline **3** (75 mg, 0.16 mmol), Ph₃CBF₄ (51
55 mg, 0.16 mmol), and anhydrous DCM (0.8 mL) was degassed under vacuum, and saturated with
56 argon (by an Ar-filled balloon) three times. The mixture was stirred for 16 hours, then diethyl ether
57
58
59
60

(1 mL) was added causing the precipitation of a solid material. Subsequent filtration and washings of the solid with fresh diethyl ether afforded the poly-(triazolium) salt **5** (62 mg) as an off-white powder partially contaminated by uncharacterized by-products. ^1H NMR (300 MHz, acetone- d_6) δ = 11.36-10.88 (m), 8.14-6.88 (m), 6.53-6.11 (m), 5.59-5.11 (m), 3.81-3.46 (m), 3.45-3.10 (m); ^{13}C NMR (101 MHz, acetone- d_6) δ = 151.7, 147.1, 146.3, 145.0, 144.4, 142.3, 141.8, 140.1, 139.5, 136.9, 135.9, 129.4, 128.1, 127.5, 126.5, 125.9, 122.2, 111.3, 77.6, 62.5, 60.0, 36.7.; ^{19}F NMR (376 MHz, acetone- d_6) δ = -146.70, -151.40, -151.45, -161.85.

Triazoline-functionalized polystyrene (PS-6).

A homogeneous mixture of styryl-triazoline derivative **3** (240 mg, 0.50 mmol), styrene (400 μL , 3.47 mmol), divinylbenzene (technical grade, 80%; 140 μL , 1.00 mmol), Toluene (211 μL , 1.98 mmol), 1-dodecanol (1.09 mL, 4.89 mmol), and AIBN (7 mg, 0.04 mmol) was degassed under vacuum, and saturated with argon (by an Ar-filled balloon) three times. The mixture was then poured into a glass column sealed at both ends (placed in vertical position) and heated at 70 $^\circ\text{C}$ in a standard oven for 24h. After cooling of the reaction column, the glass was broken, and the resulting monolith **PS-6** was triturated to obtain an orange powder. This powder was suspended in THF (5 mL) and centrifuged with portions of THF (4×5 mL). The composition of the collected supernatants was analyzed by ^1H NMR to confirm the full incorporation of the monomer **3** into the polymer. After vacuum drying (0.1 mbar, 40 $^\circ\text{C}$, 6 h), **PS-6** resin was further submitted to elemental and FT-IR analyses and the final oxidation step. Elemental analysis (%) found: N 2.80 (loading = 0.67 mmol g^{-1}). FT-IR (KBr): ν 3032 (C-H), 2920 (C-H), 1710 (C=N), 1526 (C=C), 1025 (C-N), 1000 (C-O), 712 cm^{-1} .

Triazolium-functionalized polystyrene (PS-7).

A vigorously stirred suspension of the resin **PS-6** (0.43 g, 0.29 mmol, loading = 0.67 mmol g^{-1}), Ph_3CBF_4 (0.28 g, 0.86 mmol) and anhydrous CH_3CN (1.5 mL) was degassed under vacuum, and saturated with argon (by an Ar-filled balloon) three times. The mixture was then stirred at room temperature for 16 h to give the resin **PS-7**. ^1H NMR analysis of the supernatant solution (40 μL ; dimethyl sulfone as internal standard) confirmed the quantitative oxidation of the triazoline ring by quantification of the triphenylmethane by-product. The **PS-7** resin was then centrifuged using fresh portions of CH_3CN (2×3 mL) and Et_2O (2×3 mL) and finally vacuum dried (0.1 mbar, 40 $^\circ\text{C}$, 6 h). Elemental analysis (%) found: N 2.65 (loading = 0.63 mmol g^{-1}). FT-IR (KBr): ν 3043 (C-H), 2923 (C-H), 1695 (C=N), 1530 (C=C), 1079 (C-N), 995 (C-O), 703 cm^{-1} .

Triazoline-functionalized silica (Si-6).

A stirred solution of vinylated triazoline derivative **3** (132 mg, 0.27 mmol), 3-mercaptopropyl silica gel (156 mg, 0.18 mmol, loading = 1.16 mmol g⁻¹), AIBN (42 mg, 0.18 mmol), and anhydrous toluene (1.5 mL) was degassed under vacuum, and saturated with argon (by an Ar-filled balloon) three times. The mixture was stirred and heated to 85 °C overnight. After cooling to room temperature, the mixture was centrifuged with fresh portions of THF (2 × 5 mL). The resulting silica-supported triazoline **Si-6** was finally dried (0.1 mbar, 40 °C, 6 h). Elemental analysis (%) found: N 2.02 (loading = 0.48 mmol g⁻¹). FT-IR (KBr): ν 3663 (O-H), 2931 (C-H), 1699 (C=N), 1514 (C=C), 1097 (C-O), 808 cm⁻¹.

Triazolium-functionalized silica (Si-7).

A vigorously stirred mixture of silica-supported triazoline **Si-6** (174 mg, 0.084 mmol, loading = 0.48 mmol g⁻¹), Ph₃CBF₄ (84 mg, 0.25 mmol), and anhydrous CH₃CN (2.0 mL) was degassed under vacuum, and saturated with argon (by an Ar-filled balloon) three times. The mixture was stirred at room temperature for 16 h to give the silica **Si-7**. ¹HNMR analysis of the supernatant solution (40 μ L; dimethyl sulfone as internal standard) showed a conversion of 82% of the oxidation step by quantification of the triphenylmethane by-product. The silica **Si-7** was then centrifuged with fresh portions of CH₃CN (2 × 3 mL) and Et₂O (2 × 3 mL) and finally vacuum dried (0.1 mbar, 40 °C, 6 h). Elemental analysis (%) found: N 1.85 (loading = 0.46 mmol g⁻¹). FT-IR (KBr): ν 3656 (O-H), 2942 (C-H), 1657 (C=N), 1522 (C=C), 1195 (C-N), 1079 (C-O), 808 cm⁻¹.

Screening of reaction conditions with PS-7, Si-7, and 5 leading to chromanone 9a.

Entries 1-8. A stirred mixture of **8a** (28 mg, 0.12 mmol), catalyst **PS-7** (mol% based on **8a**, loading = 0.63 mmol g⁻¹), and the stated solvent (1.0 mL) was degassed under vacuum, and saturated with argon (by an Ar-filled balloon) three times. Then, the stated base was added (mol% based on **8a**) and the reaction was stirred at room temperature for 16 h. Filtration and washing (EtOAc) of the catalyst, concentration, and elution of the resulting residue from a column of silica with 15:1 cyclohexane-EtOAc afforded **9a**.

Entry 9. A stirred mixture of **8a** (28 mg, 0.12 mmol), catalyst **PS-7** (19 mg, 0.012 mmol, loading = 0.63 mmol g⁻¹), and a 1:1 mixture of EtOH and phosphate buffer 8.5 (1.0 mL) was degassed under vacuum, and saturated with argon (by an Ar-filled balloon) three times. Then, KHMDS (24 μ L of a 0.5 M solution in anhydrous Toluene, 0.012 mmol) was added and the mixture was stirred for 16 h at room temperature. Filtration and washing (EtOAc) of the catalyst, concentration, and subsequent ¹HNMR analysis of the resulting residue confirmed the absence of **9a**.

1
2
3 *Entries 10-11.* A stirred mixture of **8a** (28 mg, 0.12 mmol), catalyst **PS-7** (mol% based on **8a**,
4 loading = 0.63 mmol g⁻¹) and anhydrous Toluene (1.0 mL) was degassed under vacuum, and
5 saturated with argon (by an Ar-filled balloon) three times. Then, KHMDS (0.5 M solution in
6 anhydrous Toluene, mol% based on **8a**) was added and the mixture was stirred for 16 h at the stated
7 temperature. Filtration and washing (EtOAc) of the catalyst, concentration, and elution of the
8 resulting residue from a column of silica with 15:1 cyclohexane-EtOAc afforded **9a**.

9
10
11
12 *Entry 12.* A stirred mixture of **8a** (28 mg, 0.12 mmol), catalyst **Si-7** (26 mg, 0.012 mmol, loading =
13 0.46 mmol g⁻¹), and anhydrous Toluene (1.0 mL) was degassed under vacuum, and saturated with
14 argon (by an Ar-filled balloon) three times. Then, KHMDS (24 μL of a 0.5 M solution in anhydrous
15 Toluene, 0.012 mmol) was added and the mixture was stirred for 16 h at the stated temperature.
16 Filtration and washing (EtOAc) of the catalyst, concentration, and elution of the resulting residue
17 from a column of silica with 15:1 cyclohexane-EtOAc afforded **9a**.

18
19
20
21
22 *Entries 13-14.* A stirred mixture of **8a** (28 mg, 0.12 mmol), catalyst **PS-7** (recycled from previous
23 cycles, 19 mg, 0.012 mmol, loading = 0.63 mmol g⁻¹), and anhydrous Toluene (1.0 mL) was
24 degassed under vacuum, and saturated with argon (by an Ar-filled balloon) three times. Then,
25 KHMDS (24 μL of a 0.5 M solution in anhydrous Toluene, 0.012 mmol) was added and the mixture
26 was stirred for 16 h at room temperature. Filtration and washing (EtOAc) of the catalyst,
27 concentration, and elution of the resulting residue from a column of silica with 15:1 cyclohexane-
28 EtOAc afforded **9a**.

29
30
31
32
33
34 *Entry 15.* A stirred mixture of **8a** (28 mg, 0.12 mmol), catalyst **5** (7 mg, 0.012 mmol based on
35 triazolium units), and anhydrous Toluene (1.0 mL) was degassed under vacuum, and saturated with
36 argon (by an Ar-filled balloon) three times. Then, KHMDS (24 μL of a 0.5 M solution in anhydrous
37 Toluene, 0.012 mmol) was added and the mixture was stirred for 16 h at room temperature.
38 Filtration and washing (EtOAc) of the catalyst, concentration, and elution of the resulting residue
39 from a column of silica with 15:1 cyclohexane-EtOAc afforded **9a**.

40 41 42 43 44 45 46 **Reaction scope with PS-7 under batch conditions.**

47 A stirred mixture of **8** (0.24 mmol), catalyst **PS-7** (38 mg, 0.024 mmol, loading = 0.63 mmol g⁻¹),
48 and anhydrous Toluene (2.0 mL) was degassed under vacuum, and saturated with argon (by an Ar-
49 filled balloon) three times. Then, KHMDS (48 μL of a 0.5 M solution in anhydrous Toluene, 0.024
50 mmol) was added and the reaction was stirred for the stated time at room temperature. Filtration and
51 washing (EtOAc) of the catalyst, concentration, and elution of the resulting residue from a column
52 of silica with the suitable elution system afforded **9**.

(R)-Ethyl 2-(4-oxochroman-3-yl)acetate (9a). Column chromatography with 15:1 cyclohexane-EtOAc afforded **9a** (53 mg, 95%) as a colorless oil. $[\alpha]_D^{25} = -11.4$ ($c = 0.5$, CH_2Cl_2); ^1H NMR (300 MHz, CDCl_3) $\delta = 7.88$ (m, 1H, H-5), 7.47 (m, 1H, H-7), 7.09-6.89 (m, 2H, H-6, H-8), 4.59 (dd, $J_{2a,2b} = 11.3$, $J_{2a,3} = 5.3$ Hz, 1H, H-2a), 4.29 (t, $J_{2b,2a-3} = 11.3$ Hz, 1H, H-2b), 4.18 (q, $J_{\text{OCH}_2, \text{CH}_3} = 7.1$ Hz, 2H, OCH_2), 3.33 (m, 1H, H-3), 2.93 (dd, $J_{\text{CH}_2\text{aCO}, \text{CH}_2\text{bCO}} = 17.0$, $J_{\text{CH}_2\text{aCO}, 3} = 4.8$ Hz, 1H, CH_2aCO), 2.41 (dd, $J_{\text{CH}_2\text{aCO}, \text{CH}_2\text{bCO}} = 17.0$, $J_{\text{CH}_2\text{bCO}, 3} = 8.2$ Hz, 1H, CH_2bCO), 1.28 (t, $J_{\text{OCH}_2, \text{CH}_3} = 7.1$ Hz, 3H, CH_3); ^{13}C NMR (101 MHz, CDCl_3) $\delta = 192.6$ (C=O), 171.4 (COOEt), 161.7 (C), 136.0 (CH), 127.4 (CH), 121.5 (CH), 120.5 (C), 117.8 (CH), 70.2 (CH_2 -2), 61.0 (OCH_2), 42.5 (CH-3), 30.3 (CH_2CO), 14.2 (CH_3); chiral HPLC analysis: 93% ee (Lux amylose 2, *n*-hexane/*i*-propanol = 96/4, flow rate 1.0 mL/min, $\lambda = 254$ nm); $t_r = 20.66$ and 25.71 min. HRMS (ESI/Q-TOF) calcd for $\text{C}_{13}\text{H}_{14}\text{NaO}_4$ ($[\text{M} + \text{Na}]^+$) 257.0784, found: 257.0732.

(R)-Ethyl 2-(6-methyl-4-oxochroman-3-yl)acetate (9b). Column chromatography with 13:1 cyclohexane-EtOAc afforded **9b** (56 mg, 95%) as a colorless oil. $[\alpha]_D^{25} = -9.3$ ($c = 1.2$, CH_2Cl_2); ^1H NMR (300 MHz, CDCl_3) $\delta = 7.66$ (d, $J_{5,7} = 1.8$ Hz, 1H, H-5), 7.28 (dd, $J_{7,8} = 8.4$, $J_{5,7} = 1.8$ Hz, 1H, H-7), 6.86 (d, $J_{7,8} = 8.4$ Hz, 1H, H-8), 4.55 (dd, $J_{2a,2b} = 11.3$, $J_{2a,3} = 5.2$ Hz, 1H, H-2a), 4.26 (t, $J_{2b,2a-3} = 11.3$ Hz, 1H, H-2b), 4.17 (q, $J_{\text{OCH}_2, \text{CH}_3} = 7.1$ Hz, 2H, OCH_2), 3.29 (m, 1H, H-3), 2.91 (dd, $J_{\text{CH}_2\text{aCO}, \text{CH}_2\text{bCO}} = 16.9$, $J_{\text{CH}_2\text{aCO}, 3} = 4.8$ Hz, 1H, CH_2aCO), 2.40 (dd, $J_{\text{CH}_2\text{aCO}, \text{CH}_2\text{bCO}} = 16.9$, $J_{\text{CH}_2\text{bCO}, 3} = 8.2$ Hz, 1H, CH_2bCO), 2.29 (s, 3H, CH_3 -6), 1.27 (t, $J_{\text{OCH}_2, \text{CH}_3} = 7.1$ Hz, 3H, CH_3); ^{13}C NMR (101 MHz, CDCl_3) $\delta = 192.8$ (C=O), 171.4 (COOEt), 159.8 (C), 137.1 (CH), 131.0 (C), 126.9 (CH), 120.1 (C), 117.6 (CH), 70.2 (CH_2 -2), 60.9 (OCH_2), 42.5 (CH-3), 30.4 (CH_2CO), 20.4 (CH_3 -6), 14.2 (CH_3); chiral HPLC analysis: 95% ee (Lux amylose 2, *n*-hexane/*i*-propanol = 96/4, flow rate 1.0 mL/min, $\lambda = 254$ nm); $t_r = 19.29$ and 25.84 min. HRMS (ESI/Q-TOF) calcd for $\text{C}_{14}\text{H}_{16}\text{NaO}_4$ ($[\text{M} + \text{Na}]^+$) 271.0941, found: 271.0985.

(R)-Ethyl 2-(6-methoxy-4-oxochroman-3-yl)acetate (9c). Column chromatography with 13:1 cyclohexane-EtOAc afforded **9c** (60 mg, 95% yield) as a colorless oil. $[\alpha]_D^{25} = -21.6$ ($c = 1.3$, CH_2Cl_2); ^1H NMR (300 MHz, CDCl_3) $\delta = 7.30$ (d, $J_{5,7} = 3.2$ Hz, 1H, H-5), 7.08 (dd, $J_{7,8} = 9.0$, $J_{5,7} = 3.2$ Hz, 1H, H-7), 6.90 (d, $J_{7,8} = 9.0$ Hz, 1H, H-8), 4.54 (dd, $J_{2a,2b} = 11.3$, $J_{2a,3} = 5.2$ Hz, 1H, H-2a), 4.25 (t, $J_{2b,2a-3} = 11.3$ Hz, 1H, H-2b), 4.17 (q, $J_{\text{OCH}_2, \text{CH}_3} = 7.1$ Hz, 2H, OCH_2), 3.78 (s, 3H, OCH_3), 3.30 (m, 1H, H-3), 2.90 (dd, $J_{\text{CH}_2\text{aCO}, \text{CH}_2\text{bCO}} = 16.9$, $J_{\text{CH}_2\text{aCO}, 3} = 4.8$ Hz, 1H, CH_2aCO), 2.41 (dd, $J_{\text{CH}_2\text{aCO}, \text{CH}_2\text{bCO}} = 16.9$, $J_{\text{CH}_2\text{bCO}, 3} = 8.2$ Hz, 1H, CH_2bCO), 1.27 (t, $J_{\text{OCH}_2, \text{CH}_3} = 7.1$ Hz, 3H, CH_3); ^{13}C NMR (101 MHz, CDCl_3) $\delta = 192.7$ (C=O), 171.4 (COOEt), 156.4 (C), 154.1 (C), 125.3 (CH), 120.2 (C), 119.1 (CH), 107.6 (CH), 70.3 (CH_2 -2), 61.0 (OCH_2), 55.8 (OCH_3), 42.5 (CH-3), 30.5 (CH_2CO), 14.2 (CH_3); chiral HPLC analysis: 90% ee (Lux amylose 2, *n*-hexane/*i*-propanol = 96/4,

1
2
3 flow rate 1.0 mL/min, $\lambda = 254$ nm); $t_r = 30.94$ and 35.93 min. HRMS (ESI/Q-TOF) calcd for
4 $C_{14}H_{16}NaO_5$ ($[M + Na]^+$) 287.0890, found: 287.0867.

5
6 **(R)-Ethyl 2-(6-chloro-4-oxochroman-3-yl)acetate (9d)**. Column chromatography with 12:1
7 cyclohexane-EtOAc afforded **9d** (61 mg, 95% yield) as a colorless oil. $[\alpha]_D^{25} = -16.7$ ($c = 0.9$,
8 CH_2Cl_2); 1H NMR (300 MHz, $CDCl_3$) $\delta = 7.83$ (d, $J_{5,7} = 2.7$ Hz, 1H, H-5), 7.41 (dd, $J_{7,8} = 8.9$, $J_{5,7} =$
9 2.7 Hz, 1H, H-7), 6.93 (d, $J_{7,8} = 8.9$ Hz, 1H, H-8), 4.60 (dd, $J_{2a,2b} = 11.3$, $J_{2a,3} = 5.3$ Hz, 1H, H-2a),
10 4.26 (t, $J_{2b,2a-3} = 11.3$ Hz, 1H, H-2b), 4.15 (q, $J_{OCH_2,CH_3} = 7.2$ Hz, 2H, OCH_2), 3.28 (m, 1H, H-3),
11 2.91 (dd, $J_{CH_2aCO,CH_2bCO} = 17.1$, $J_{CH_2aCO,3} = 4.7$ Hz, 1H, CH_2aCO), 2.42 (dd, $J_{CH_2aCO,CH_2bCO} = 17.1$,
12 $J_{CH_2bCO,3} = 8.1$ Hz, 1H, CH_2bCO), 1.27 (t, $J_{OCH_2,CH_3} = 7.2$ Hz, 3H, CH_3); ^{13}C NMR (101 MHz,
13 $CDCl_3$) $\delta = 191.6$ (C=O), 171.1 (COOEt), 160.2 (C), 135.8 (CH), 127.0 (C), 126.7 (CH), 121.2 (C),
14 119.6 (CH), 70.3 (CH_2-2), 61.1 (OCH_2), 42.3 (CH-3), 30.2 (CH_2CO), 14.2 (CH_3); chiral HPLC
15 analysis: 92% ee (Lux cellulose 2, *n*-hexane/*i*-propanol = 95/5, flow rate 0.5 mL/min, $\lambda = 254$ nm);
16 $t_r = 10.07$ and 11.11 min. HRMS (ESI/Q-TOF) calcd for $C_{13}H_{13}ClNaO_4$ ($[M + Na]^+$) 291.0395,
17 found: 291.0412.

18
19 **(R)-Ethyl 2-(6-bromo-4-oxochroman-3-yl)acetate (9e)**. Column chromatography with 12:1
20 cyclohexane-EtOAc afforded **9e** (71 mg, 95% yield) as a colorless oil. $[\alpha]_D^{25} = -11.24$ ($c = 1.5$,
21 CH_2Cl_2); 1H NMR (300 MHz, $CDCl_3$) $\delta = 7.97$ (d, $J_{5,7} = 2.5$ Hz, 1H, H-5), 7.53 (dd, $J_{7,8} = 8.8$, $J_{5,7} =$
22 2.5 Hz, 1H, H-7), 6.87 (d, $J_{7,8} = 8.8$ Hz, 1H, H-8), 4.59 (dd, $J_{2a,2b} = 11.3$, $J_{2a,3} = 5.4$ Hz, 1H, H-2a),
23 4.28 (t, $J_{2b,2a-3} = 11.3$ Hz, 1H, H-2b), 4.15 (q, $J_{OCH_2,CH_3} = 7.2$ Hz, 2H, OCH_2), 3.28 (m, 1H, H-3),
24 2.90 (dd, $J_{CH_2aCO,CH_2bCO} = 17.0$, $J_{CH_2aCO,3} = 4.7$ Hz, 1H, CH_2aCO), 2.41 (dd, $J_{CH_2aCO,CH_2bCO} = 17.0$,
25 $J_{CH_2bCO,3} = 8.1$ Hz, 1H, CH_2bCO), 1.27 (t, $J_{OCH_2,CH_3} = 7.2$ Hz, 3H, CH_3); ^{13}C NMR (101 MHz,
26 $CDCl_3$) $\delta = 191.4$ (C=O), 171.1 (COOEt), 160.6 (C), 138.6 (CH), 129.8 (CH), 121.7 (C), 119.9
27 (CH), 114.16 (C), 70.3 (CH_2-2), 61.1 (OCH_2), 42.2 (CH-3), 30.2 (CH_2CO), 14.2 (CH_3); chiral
28 HPLC analysis: 92% ee (Lux cellulose 2, *n*-hexane/*i*-propanol = 97/3, flow rate 0.5 mL/min, $\lambda =$
29 254 nm); $t_r = 12.82$ and 14.15 min. HRMS (ESI/Q-TOF) calcd for $C_{13}H_{13}BrNaO_4$ ($[M + Na]^+$)
30 334.9889, found: 334.9855.

31
32 **(R)-Ethyl 2-(8-methyl-4-oxochroman-3-yl)acetate (9f)**. Column chromatography with 14:1
33 cyclohexane-EtOAc afforded **9f** (57 mg, 95% yield) as a colorless oil. $[\alpha]_D^{25} = -8.95$ ($c = 1.3$,
34 CH_2Cl_2); 1H NMR (300 MHz, $CDCl_3$) $\delta = 7.73$ (dd, $J_{5,6} = 7.8$, $J_{5,7} = 0.9$ Hz, 1H, H-5), 7.33 (dd,
35 $J_{6,7} = 7.8$, $J_{5,7} = 0.9$ Hz, 1H, H-7), 6.91 (t, $J_{6,5-7} = 7.8$ Hz, 1H, H-6), 4.63 (dd, $J_{2a,2b} = 11.3$, $J_{2a,3} = 5.3$
36 Hz, 1H, H-2a), 4.28 (t, $J_{2b,2a-3} = 11.3$ Hz, 1H, H-2b), 4.18 (q, $J_{OCH_2,CH_3} = 7.1$ Hz, 2H, OCH_2), 3.30
37 (m, 1H, H-3), 2.93 (dd, $J_{CH_2aCO,CH_2bCO} = 16.9$, $J_{CH_2aCO,3} = 4.8$ Hz, 1H, CH_2aCO), 2.39 (dd,
38 $J_{CH_2aCO,CH_2bCO} = 16.9$, $J_{CH_2bCO,3} = 8.2$ Hz, 1H, CH_2bCO), 2.23 (s, 3H, CH_3-8), 1.28 (t, $J_{OCH_2,CH_3} = 7.1$
39 Hz, 3H, CH_3); ^{13}C NMR (101 MHz, $CDCl_3$) $\delta = 193.0$ (C=O), 171.5 (COOEt), 160.0 (C), 136.8
40
41
42
43
44
45

(CH), 127.1 (C), 124.9 (CH), 120.9 (CH), 120.1 (C), 70.31 (CH₂-2), 61.0 (OCH₂), 42.3 (CH-3), 30.4 (CH₂CO), 15.6 (CH₃-8), 14.2 (CH₃); chiral HPLC analysis: 81% ee (Lux amylose 2, *n*-hexane/*i*-propanol = 95/5, flow rate 1.0 mL/min, λ = 254 nm); t_r = 16.20 and 17.73 min. HRMS (ESI/Q-TOF) calcd for C₁₄H₁₆NaO₄ ([M + Na]⁺) 271.0941, found: 271.0978.

(R)-Ethyl 2-(8-methoxy-4-oxochroman-3-yl)acetate (9g). Column chromatography with 15:1 cyclohexane-EtOAc afforded **9g** (60 mg, 95% yield) as a colorless oil. $[\alpha]_D^{25}$ = -23.5 (c = 1.2, CH₂Cl₂); ¹H NMR (300 MHz, CDCl₃) δ = 7.47 (dd, $J_{5,6}$ = 7.9, $J_{5,7}$ = 1.6 Hz, 1H, H-5), 7.04 (dd, $J_{6,7}$ = 7.9, $J_{5,7}$ = 1.6 Hz, 1H, H-7), 6.95 (t, $J_{6,5-7}$ = 7.9 Hz, 1H, H-6), 4.69 (dd, $J_{2a,2b}$ = 11.3, $J_{2a,3}$ = 5.2 Hz, 1H, H-2a), 4.36 (t, $J_{2b,2a-3}$ = 11.3 Hz, 1H, H-2b), 4.17 (q, J_{OCH_2,CH_3} = 7.1 Hz, 2H, OCH₂), 3.89 (s, 3H, OCH₃), 3.33 (m, 1H, H-3), 2.89 (dd, J_{CH_2aCO,CH_2bCO} = 17.0, $J_{CH_2aCO,3}$ = 4.9 Hz, 1H, CH_{2a}CO), 2.43 (dd, J_{CH_2aCO,CH_2bCO} = 17.0, $J_{CH_2bCO,3}$ = 8.1 Hz, 1H, CH_{2b}CO), 1.26 (t, J_{OCH_2,CH_3} = 7.1 Hz, 3H, CH₃); ¹³C NMR (101 MHz, CDCl₃) δ = 192.5 (C=O), 171.2 (COOEt), 170.7 (C), 151.6 (C), 148.7 (C), 121.0 (CH), 118.5 (CH), 116.6 (CH), 70.7 (CH₂-2), 61.0 (OCH₂), 56.2 (OCH₃), 42.4 (CH-3), 30.3 (CH₂CO), 14.2 (CH₃); chiral HPLC analysis: 90% ee (Lux amylose 2, *n*-hexane/*i*-propanol = 65/35, flow rate 1.0 mL/min, λ = 254 nm); t_r = 20.73 and 30.69 min. HRMS (ESI/Q-TOF) calcd for C₁₄H₁₆NaO₅ ([M + Na]⁺) 287.0890, found: 287.0825

Fabrication of monolithic microreactor (MM-7)

A homogeneous mixture of **3** (191 mg, 0.39 mmol), styrene (319 μ L, 2.76 mmol), divinylbenzene (technical grade, 80%; 111 μ L, 0.79 mmol), Toluene (168 μ L, 1.63 mmol), 1-dodecanol (871 μ L, 3.87 mmol), and AIBN (6 mg, 0.04 mmol) was degassed under vacuum, and saturated with argon (by an Ar-filled balloon) three times. The mixture was then poured in a stainless-steel column (length: 10 cm, 0.46 cm internal diameter) sealed at both ends, and placed in a vertical position in a standard convection oven. The polymerization was allowed to proceed for 24 h at 70 °C, then the column **MM-6** was cooled to room temperature and the seals removed. The column was provided with fittings, connected to the HPLC pump, and warmed to 50 °C. Then, THF was pumped through the warmed column at a flow rate of 50 μ L min⁻¹ for 5 h to remove the porogenic solvents and residual non-polymeric materials. The column **MM-6** was cooled to room temperature and then an input stream of a 0.5 M solution of Ph₃CBF₄ in anhydrous CH₃CN (2 mL) was pumped at 50 μ L min⁻¹ inside the column to completely fill the microreactor (V_0 = 1.32 mL). The pump was then stopped, the column sealed at both ends, and the oxidation step was allowed to proceed for 16 h. Then the sealed were removed and the column was provided with fittings, connected to the HPLC pump, and washed at room temperature with THF at a flow rate of 50 μ L min⁻¹ for 2 h. The above stop-flow procedure was repeated other two times to give **MM-7**.

1
2
3 The same procedure for the fabrication of **MM-7** was performed with a reference microreactor in a
4 parallel experiment for SEM (Figure 2) and element analyses. Elemental analysis (%) found: N 2.65
5 (loading = 0.63 mmolg⁻¹).
6
7

8 9 **Determination of microreactor void-volume**

10
11 Microreactor void volume (V_0) was determined by pycnometry³⁴ as described before.³⁵ This method
12 consists in filling the microreactor successively with two distinct solvents (solvent 1: water; solvent
13 2: *n*-hexane) and weighing the filled microreactors accurately. Simple math shows that:³⁴
14
15

$$16 \quad V_0 = (\omega_1 - \omega_2) / (\delta_1 - \delta_2).$$

17
18 where ω_1 and ω_2 are the weights of the microreactor filled with solvents 1 and 2 and δ_1 and δ_2 the
19 densities of the solvents.
20
21

22 23 **Experimental set-up for the flow synthesis of chromanones 9.**

24
25 The system used for the flow-reaction was made of two binary pumps (Agilent 1100 and Agilent
26 1100 micro series). Channel-A was used to deliver a continuously degassed solution of **8** (0.2 M) in
27 Toluene. Channel-B delivered a continuously degassed solution of Et₃N (0.4 M) in Toluene. The
28 feed solutions were pumped at the stated flow rate through the 3-way valve into **MM-7**. The
29 microreactor was operated for 5 h under steady-state conditions, then the collected solution was
30 concentrated, and eluted from a column of silica gel with the suitable elution system to give **9**.
31
32

33
34 The long-term stability experiment was performed using aldehyde **8a** (0.4 M); microreactor **MM-7**
35 was operated at 25 °C with a flow rate of 10 $\mu\text{L min}^{-1}$ for ca. 150 h. After the achievement of the
36 steady-state regime (ca. 3 h), 90% conversion of **8a** was maintained for 48 h, while a progressive
37 loss of catalytic activity was observed after that time ($\text{TON}_{\text{flow}} = 132$).
38
39
40
41

42 43 **Ethyl benzo[b]oxepine-4-carboxylate (10a).**

44
45 Channel-A of the flow apparatus was used to deliver a continuously degassed solution of **8a** (0.2 M)
46 in Toluene. Channel-B delivered a continuously degassed solution of KHMDS (0.1 M) in Toluene.
47 The feed solutions were pumped at 10 μLmin^{-1} through the 3-way valve into **MM-7**. The
48 microreactor was operated for 5 h under steady-state conditions, then the collected solution was
49 concentrated, and eluted from a column of silica gel with 15:1 cyclohexane-EtOAc to give **10a** (57
50 mg, 88%) as yellow oil. ¹H NMR (300 MHz, CDCl₃) δ = 7.62-7.44 (m, 3H, 2Ar+H-2), 7.35 (m, 1H,
51 Ar), 7.24 (m, 1H, Ar), 6.92 (s, 1H, H-5), 6.57 (d, $J_{3,2} = 15.7$ Hz, 1H, H-3), 4.27 (q, $J_{\text{OCH}_2, \text{CH}_3} = 7.1$
52 Hz, 2H, OCH₂), 1.34 (t, $J_{\text{OCH}_2, \text{CH}_3} = 7.1$ Hz, 3H, CH₃); ¹³C NMR (101 MHz, CDCl₃) δ = 166.7
53 (COOEt), 155.5 (C), 152.3 (C), 131.2 (CH), 128.3 (C), 126.4 (CH), 123.3 (CH), 121.7 (CH), 119.0
54
55
56
57
58
59
60

(CH), 111.4 (CH), 111.0 (CH), 60.7 (OCH₂), 14.3 (CH₃). HRMS (ESI/Q-TOF) calcd for C₁₃H₁₂NaO₃ ([M + Na]⁺) 239.0679, found: 239.0625.

Supporting Information: Copies of NMR and FT-IR spectra and HPLC chromatograms.

Acknowledgment: We gratefully acknowledge the University of Ferrara (fondi FAR) for financial support. Thanks are also given to Mr Paolo Formaglio for NMR experiments, to Dr Tatiana Bernardi for HRMS analyses, and to Mrs Ercolina Bianchini for elemental analyses.

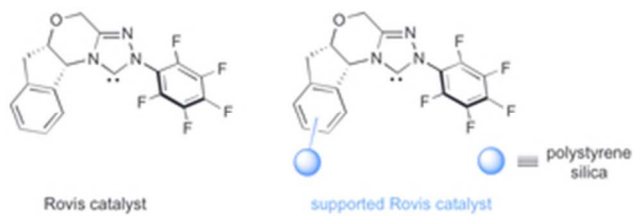
References

1. For reviews, see: (a) Nair, V.; Bindu, S.; Sreekumar, V. *Angew. Chem., Int. Ed.* **2004**, 43, 5130-5135. (b) Enders, D.; Niemeier, O.; Henseler, A. *Chem. Rev.* **2007**, 107, 5606-5655. (c) Marion, N.; Díez-Gonzalez, S.; Nolan, S. P. *Angew. Chem., Int. Ed.* **2007**, 46, 2988-3000. (d) Bugaut, X.; Glorius, F. *Chem. Soc. Rev.* **2012**, 41, 3511-3522. (e) Mahatthananchai, J.; Bode, J. W. *Acc. Chem. Res.* **2014**, 47, 696-707. (f) Flanigan, D.M.; Romanov-Michailidis, F.; White, N. A.; Rovis, T. *Chem. Rev.* **2015**, 115, 9307-9387. (g) Menon, R.S.; Biju, A.T.; Nair, V. *Chem. Rev.* **2015**, 44, 5040-5052. (h) Ren, Q.; Li, M.; Yuan, L.; Wang, J. *Org. Biomol. Chem* **2017**, 15, 4731-4749.
2. Izquierdo, J.; Huston, G. E.; Cohen, D.T.; Scheidt, A.K. *Angew. Chem. Int. Ed.* **2012**, 51, 2-15.
3. (a) Kirschning, A.; Solodenko, W.; Mennecke, K. *Chem Eur.J.* **2006**, 12, 5972-5990. (b) Bogdan A. R.; Mason, B. P.; Sylvester, K. T., McQuade, D. T. *Angew. Chem. Int. Ed.* **2007**, 46, 1698-1701. (c) Frost, C.G.; Mutton, L. *Green Chem.* **2010**, 12, 1687-1703. (d) Tsubogo, T.; Ishiwata, T.; Kobayashi, S. *Angew. Chem. Int. Ed.* **2013**, 52, 6590-6604. (e) Puglisi, A.; Benaglia, M.; Chiroli, V. *Green Chem.* **2013**, 15, 1790-1813. (e) Atodiresei, I.; Vila, C.; Rueping, M. *ACS Catal.* **2015**, 1972-1985. (f) Finelli, F. G.; Miranda, L. S. M.; de Souza, R. O. M. A. *Chem. Commun.* **2015**, 51, 3708-3722. (g) Porta, R.; Benaglia, M.; Puglisi, A. *Org. Res. Dev.* **2016**, 20, 2-25. (h) Clot-Almenara, L.; Rodríguez-Esrich, C.; Osorio-Planes, L.; Pericàs, M. A. *ACS Catal.* **2016**, 6, 7647-7651. (i) Britton, J.; Raston, C. L.

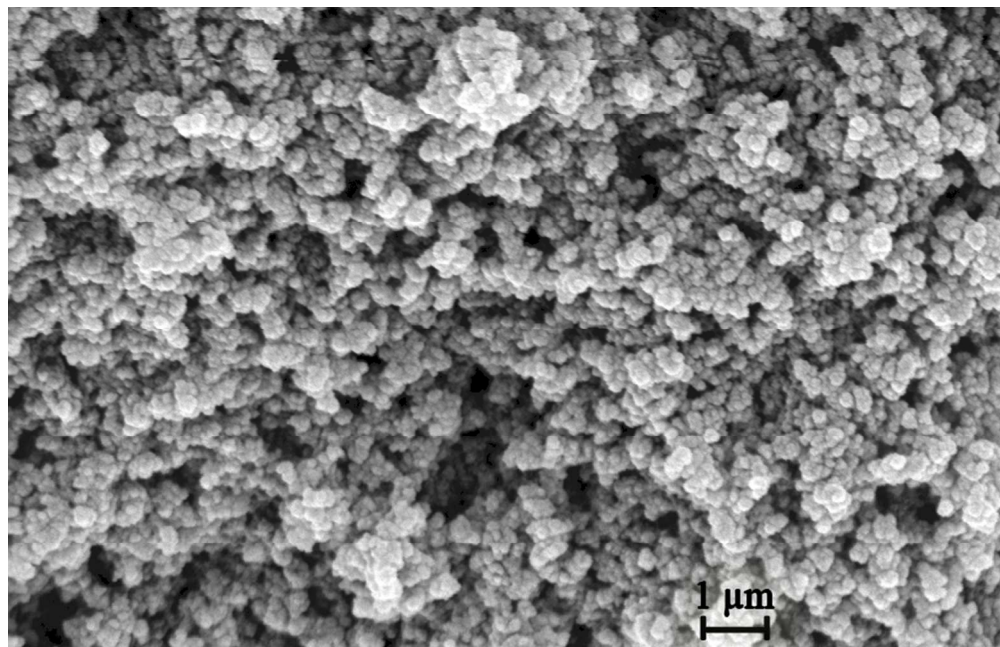
- 1
2
3 *Chem. Rev.* **2017**, 46, 1250. (j) Plutschack, M. B.; Pieber, B.; Gilmore, K.; Seeberger, P. H.
4
5 *Chem. Rev.* **2017**, article ASAP (10.1021/acs.chemrev.7b00183).
6
7
8 4. (a) Roberge, D. M.; Ducry, L.; Bieler, N.; Cretton, P.; Zimmermann, B. *Chem. Eng.*
9
10 *Technol.* **2005**, 28, 318-323. (b) Roberge, D. M.; Zimmermann, B.; Rainone, F.; Gottsponer,
11
12 M.; Eyholzer, M.; Kockmann, N. *Org. Process Res. Dev.* **2008**, 12, 905-910. (c) Pastre, J.
13
14 C.; Browne, D. L.; Ley, S. V. *Chem. Soc. Rev.* **2013**, 42, 8849-8869. (d) Hessel, V.;
15
16 Kralisch, D.; Kockmann, N.; Noël, T.; Wang, Q. *ChemSusChem* **2013**, 6, 746-789.
17
18
19 5. Zhong, R.; Lindhorst, A. C.; Groche, F. J.; Kühn, F.E. *Chem. Rev.* **2017**, 117,1970-2058.
20
21 6. Barrett, A. G.; Love, A. C.; Tedeschi, L. *Org. Lett* **2004**, 6 19, 3377-3380.
22
23 7. Storey, J. M.; Williamson, C. *Tetrahedron Lett.* **2005**, 7337-7339.
24
25 8. Zietler, K.; Mager, I. *Adv. Synth. Catal.* **2007**, 349, 1851-1857.
26
27 9. Tan, M.; Zhang, Y.; Ying, J. Y. *Adv. Synth. Catal.* **2009**, 351, 1390-1394.
28
29
30 10. Seo, U. R.; Chung, T. K. *RSC Adv.* **2014**, 4, 32371-32374.
31
32 11. Powell, A. B.; Suzuki, Y.; Ueda, M.; Bielawski, C. W.; Cowley, A. H. *J. Am. Chem. Soc.*
33
34 **2011**, 133, 5218-5220.
35
36 12. Rose, M; Notzon, A.; Heitbaum, M; Nickerl, G.; Paasch, S.; Brunner, E.; Glorius, F.;
37
38 Kaskel, S. *Chem. Commun.* **2011**, 47, 4814-4816.
39
40 13. (a) Pinaud, J.; Vignolle, J.; Gnanou, Y.; Taton, D. *Macromolecules* **2011**, 44, 1900-1908. (b)
41
42 Coupillaud, P.; Pinaud, J.; Guidolin, N.; Vignolle, J.; Fèvre, M.; Veaudecenne, E.;
43
44 Mecerreys, D.; Taton, D. *J. Polym. Sci. Part A: Polym Chem.* **2013**, 51, 4530-4540. (c)
45
46 Kuzmicz, D.; Coupillaud, P.; Men, Y.; Vignolle, J.; Vendraminetto, G.; Ambroggi, M.;
47
48 Taton, D.; Yuan, J. *Polymer* **2014**, 55, 3423-3430.
49
50
51 14. Molina de la Torre, J. A.; Albeniz, A. C. *ChemCatChem* **2014**, 6, 3547-3552.
52
53 15. Wang, L.; Chen, E. Y. X. *ACS Catal.* **2015**, 5, 6907-6917.
54
55 16. Ranganath, K. V. S.; Schäfer, A. H.; Glorius, F. *ChemCatChem* **2011**, 3, 1889-1891.
56
57 17. Di Marco, L; Hans, M.; Delaude, L.; Monbaliu, J. M. *Chem. Eur. J.* **2016**, 22, 4508-4514.
58
59
60

- 1
2
3 18. (a) Green, R. A.; Pletcher, D.; Leach, S. G.; Brown, R. C. D. *Org. Lett.* **2015**, 17, 3290-
4 3293. (b) Green, R. A.; Pletcher, D.; Leach, S. G.; Brown, R. C. D. *Org. Lett.* **2016**, 18,
5 1198-1201.
6
7
8
9
10 19. Asadi, M.; Hooper, J. F.; Lupton, D. W. *Tetrahedron* **2016**, 72, 3729-3733.
11
12 20. Bortolini, O.; Cavazzini, A.; Dambruoso, P.; Giovannini, P. P.; Caciolli, L.; Massi, A.;
13 Pacifico, S.; Ragno, D. *Green Chem.* **2013**, 15, 2981-2992.
14
15 21. Giovannini, P. P.; Bortolini, O.; Cavazzini, A.; Greco, R.; Fantin, G.; Massi, A. *Green*
16 *Chem.* **2014**, 16, 3904-3915.
17
18 22. Zaghi, A.; Ragno, D.; Di Carmine, G.; De Risi, C.; Bortolini, O.; Giovannini, P. P.; Fantin
19 G.; Massi, A. *Beilstein J. Org. Chem.* **2016**, 12, 2719-2730.
20
21 23. Selected examples: (a) Kerr, S. M.; Read de Alaniz, J.; Rovis, T. *J. Org. Chem.* **2005**, 70,
22 5725-5728. (b) Struble, J. R.; Kaeobamrung, J.; Bode, J. W. *Org. Lett.* **2008**, 5, 957-960. (c)
23 Di Rocco, D.; Oberg, K. M.; Dalton, D. M.; Rovis, T. *J. Am. Chem. Soc.* **2009**, 131, 10872-
24 10874. (d) Vora, H. U.; Rovis, T. *J. Am. Chem. Soc.* **2010**, 132, 2860-2861. (e) Mao, H.;
25 An, S. L.; Kim, S. K.; Yang, J. W. *Bull. Korean Chem. Soc.* **2011**, 32, 12, 4408-4410. (f)
26 Kuwano, S.; Harada, S.; Kang, B.; Oriez, R.; Yamaoka, Y.; Takasu, K.; Yamada, K. *J. Am.*
27 *Chem. Soc.* **2013**, 135, 11485-11488.
28
29 24. (a) van den Berg, H. J.; Challa, G.; Pandit, U. K. *J. Mol. Catal.* **1989**, 51, 13-27. (b) van den
30 Berg, H. J.; Challa, G.; Pandit, U. K. *React. Polym.* **1989**, 11, 127-134.
31
32 25. Hsieh, S.; Binanzer, M.; Kreituss, I.; Bode, J. W. *Chem. Commun.* **2012**, 48, 8892-8894.
33
34 26. Ozboya, K. E.; Rovis, T. *Synlett* **2014**, 25, 2665-2668.
35
36 27. Vora, H. U.; Lathrop, S. P.; Reynolds, N. T.; Kerr, M. S., Read de Alaniz, J.; Rovis, T. *Org.*
37 *Synth.* **2010**, 87, 350-361.
38
39 28. Bildstein, B.; Malaun, M.; Kopacka, H.; Ongania, K.; Wurst, K. *J. Organomet. Chem.* **1999**,
40 572, 177-187.
41
42 29. (a) Peters, E. C.; Svec, F.; Fréchet, J. M. *Adv. Mater.* **1999**, 11, 1169-1181. (b) Heck, R. M.;
43 Gulati, S.; Farratu, R. J. *Chem. Eur. J.* **2001**, 82, 149-156. (c) Ceylan, S; Kirschning, A. In
44
45
46
47
48
49
50
51
52
53
54
55
56
57
58
59
60

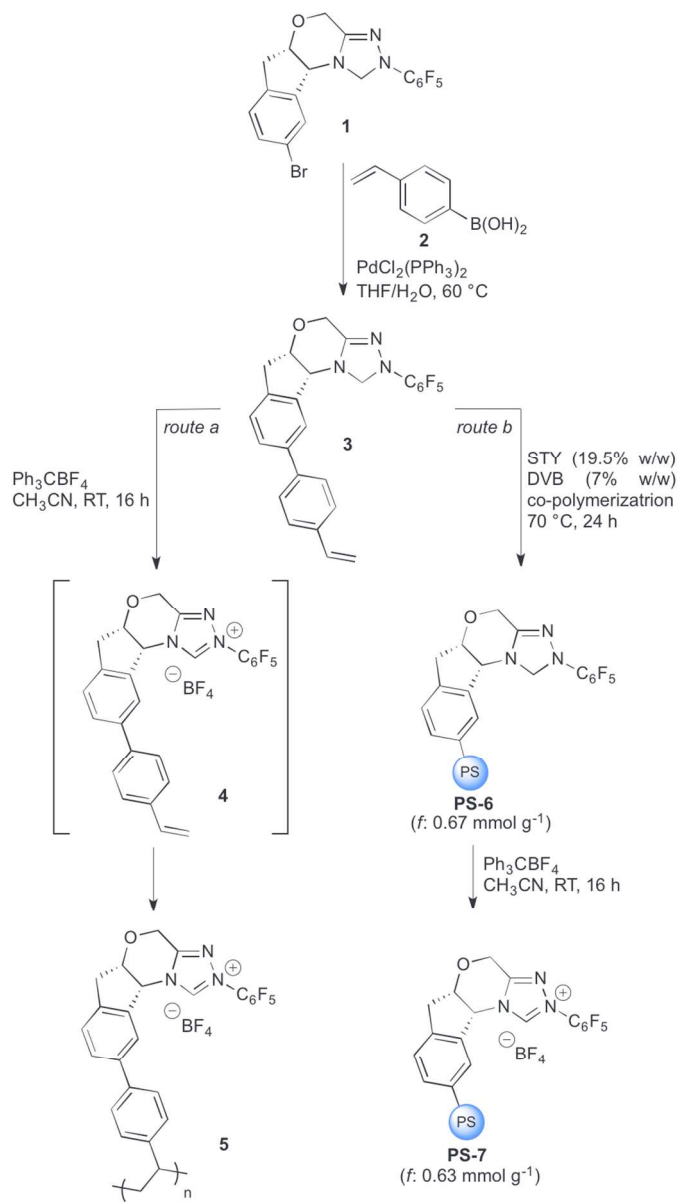
- 1
2
3 *Recoverable and Recyclable Catalysts*, M. Benaglia, Ed.; John Wiley and Sons: New York,
4 2009, p 379-403. For reports on monolithic microreactors, see: (d) Ingham, R. J.; Riva, E.;
5 Nibkin, N.; Baxendale, I. R.; Ley, S. V. *Org. Lett.* **2012**, 14, 3920-3923 and references
6 therein. (e) Lange, H.; Capener, M. J.; Jones, A. X.; Smith, C. J.; Nibkin, N.; Baxendale, I.
7 R.; Ley, S. V. *Synlett* **2011**, 869-873. (f) Ngamson, B.; Hickey, A. M.; Greenway, G. M.;
8 Littlechild, J. A.; Watts, P.; Wiles, C. *J. Mol. Catal. B: Enzym.* **2010**, 63, 81-86.
- 9
10
11
12
13 30. (a) Jas, G.; Kirschning, A. *Chem. Eur. J.* **2003**, 9, 5708-5723. (b) Stankiewicz, A. *Chem.*
14 *Eng. Sci.* **2001**, 56, 359-361.
- 15
16
17 31. Bortolini, O.; Caciolli, L.; Cavazzini, A.; Costa, V.; Greco, R.; Massi, A.; Pasti, L. *Green.*
18 *Chem.* **2012**, 14, 992-1000.
- 19
20 32. Selected papers: (a) Ciganek, E. *Synthesis* **1995**, 1311-1314. (b) Kerr, M. S.; Read de
21 Alaniz, J.; Rovis, T. *J. Am. Chem. Soc.* **2002**, 124, 10298-10299. (c) Kerr, M. S.; Rovis, T.
22 *Synlett* **2003**, 12, 1934-1936. (d) Kerr, M. S.; Rovis, T. *J. Am. Chem. Soc.* **2004**, 126, 8876-
23 8877. (e) Moore, J. L., Kerr, Mark. S.; Rovis, T. *Tetrahedron* **2006**, 62, 11477-11482. (f)
24 Read de Alaniz, J.; Kerr, M. S.; Moore, J. L.; Rovis, T. *J. Org. Chem.* **2008**, 73, 2033-2040.
25 (g) Read de Alaniz, J.; Rovis, T. *Synlett* **2009**, 8, 1189-1207. (h) Moore, J. L.; Silvestri, A.
26 P.; Read de Alaniz, J.; DiRocco, D. A.; Rovis, T. *Org. Lett.* **2011**, 13, 7, 1742-1745.
- 27
28
29
30
31 33. Youn, S.W; Song, H. S.; Park, J. H. *Org. Biomol. Chem.* **2014**, 12, 2388-2393.
- 32
33 34. McCormick R. M.; Karger, B. L. *Anal. Chem.* **1980**, 52, 2249-2257.
- 34
35 35. Gritti, F.; Kazakevich Y.; Guiochon, G. *J. Chromatogr. A* **2007**, 1161, 157-169.
- 36
37
38
39
40
41
42
43
44
45
46
47
48
49
50
51
52
53
54
55
56
57
58
59
60



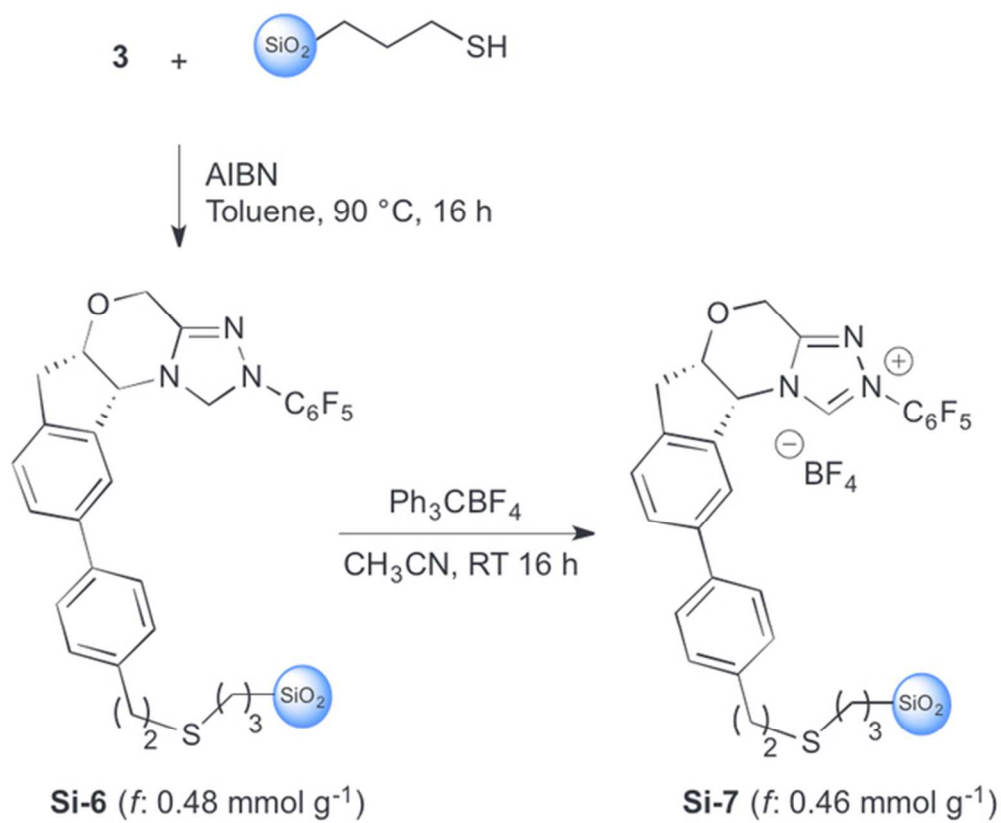
26x8mm (300 x 300 DPI)



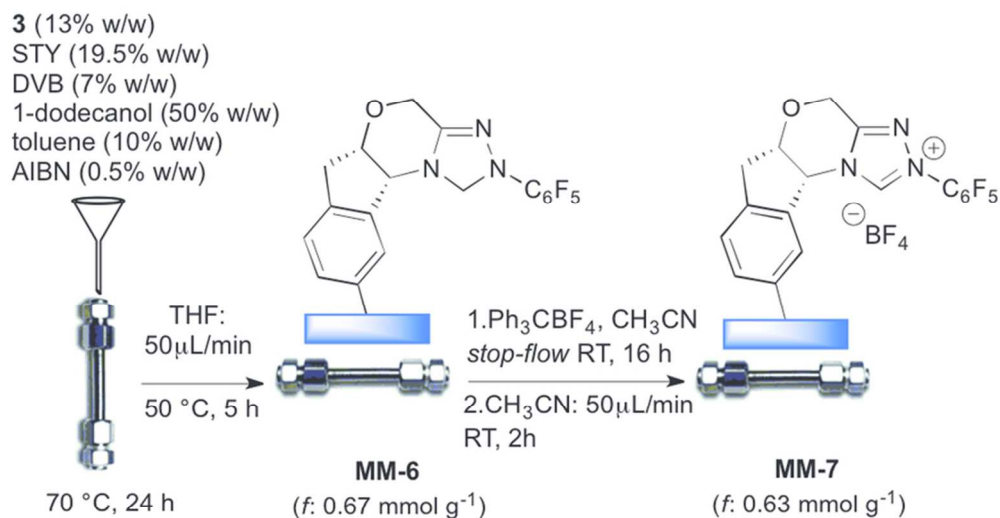
354x227mm (72 x 72 DPI)



79x141mm (300 x 300 DPI)



55x45mm (300 x 300 DPI)

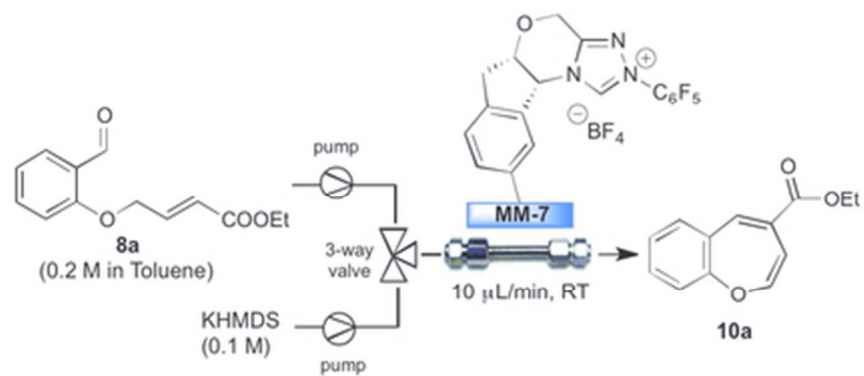


	loaded 3 [mmol] ^a	V_G [mL] ^b	V_o [mL] ^c	Total Porosity ^d	Time [min] ^e	Pressure [bar] ^f
MM-7	0.40	1.66	1.32	0.80	132	2

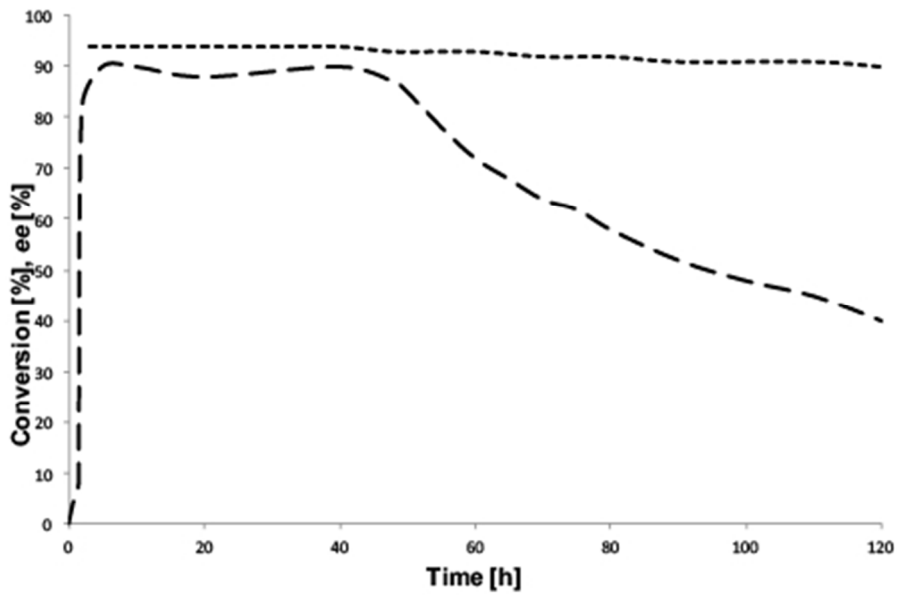
^aDetermined by elemental analysis and expressed as mmol of pyrrolidinyl-tetrazole units per gram of functionalized resin.

^bGeometric volume of the stainless-steel column. ^cVoid volume determined by pycnometry. ^dTotal porosity = V_o/V_G . ^eResidence time calculated at 10 μLmin^{-1} . ^fBackpressure measured at 20 μLmin^{-1} (RT, THF).

74x67mm (300 x 300 DPI)



36x15mm (300 x 300 DPI)



79x52mm (144 x 144 DPI)

